(8) Poland, D.; Scheraga, H. A. "Theory of Helix–Coil Transitions in Biopolymers"; Academic Press: New York, 1970.
(9) Mattice, W. L.; Scheraga, H. A. *Polym. Prepr., Div. Polym. Chem., Am. Chem. Soc.* **1984**, *25*, 276.
(10) Abe, A.; Jernigan, R. L.; Flory, P. J. *J. Am. Chem. Soc.* **1966**, *88*, 631.
(11) Flory, P. J. *Macromolecules* **1974**, *7*, 381.
(12) Némethy, G.; Scheraga, H. A. *Q. Rev. Biophys.* **1977**, *10*, 239.

Double-Stranded Helix of Xanthan: Dimensional and Hydrodynamic Properties in 0.1 M Aqueous Sodium Chloride

Takahiro Sato, Takashi Norisuye,* and Hiroshi Fujita

Department of Macromolecular Science, Osaka University, Toyonaka, Osaka 560, Japan.
Received June 1, 1984

ABSTRACT: Sedimentation velocity data were obtained for 12 samples of xanthan (sodium salt) in 0.1 M aqueous NaCl at 25 °C, in which this polysaccharide dissolves as a double helix. For two of these samples, light scattering and viscosity data in the same solvent were obtained and combined with the previous data for other samples. The limiting sedimentation coefficients, radii of gyration, and intrinsic viscosities as functions of weight-average molecular weight M_w showed the double helix of xanthan in 0.1 M aqueous NaCl to be almost completely rigid below and semiflexible above $M_w \sim 3 \times 10^5$. Analysis of these data in terms of the known theories for rods and wormlike chains yielded 0.47 ± 0.02, 2.4 ± 0.3, and 120 ± 20 nm for the pitch h (per main-chain glucose residue), diameter d, and persistence length of the xanthan double helix, respectively. These h and d values agreed with those reported for crystalline xanthan, confirming the previous conclusion that the double-helical structure of the polysaccharide in 0.1 M aqueous NaCl is essentially the same as that in the crystalline state.

Introduction

Xanthan is an ionic, extracellular polysaccharide produced by the bacterium *Xanthomonas campestris*. It consists of a main chain of β-1,4-linked D-glucoses and three sugar side chains attached to every other main-chain residue.[1,2] In recent papers,[3,4] we concluded from light scattering and viscosity measurements that xanthan (sodium salt) dissolves in 0.1 M aqueous sodium chloride (NaCl) as rodlike dimers having essentially the same double-stranded helical structure as that proposed by Okuyama et al.[5] for crystalline xanthan.

To confirm this conclusion from another angle the limiting sedimentation coefficient was measured on 12 samples of xanthan sodium salt in 0.1 M aqueous NaCl. Further, light scattering and viscosity measurements were made on two of these samples in the same solvent, since they had not been treated in our previous work.[3,4]

In this paper, all the data from the present and previous experiments were combined to redetermine the pitch, diameter, and rigidity (expressed in terms of the persistence length) of the xanthan double helix in 0.1 M aqueous NaCl.

Experimental Section

Samples. Twelve fractionated, purified samples of xanthan (X4-5, X5-6, X5-8, X3-5, X9-3, X7-3b, X6-3-7, X6-4-4, X10-4, X6-4-7, X8-3-5, and X8-3-8) were chosen from our stock for sedimentation velocity determination. Among these, samples X5-8 and X6-4-7 were the objects of new light scattering and viscosity measurements. Sample X4-5 was extracted directly from a commercial sample (Kelco Keltrol), while the others were all obtained by sonicating the commercial sample.[3,4] Each of these samples was converted to an almost completely substituted Na salt, and 0.1 M aqueous NaCl solutions of the polysalts were prepared by the method[3] described previously. The degree of pyruvation (DS_{pyr}) ranged from 0.32 to 0.37 with no systematic variation with the molecular weight of the sample.[6] The ratios of the z-average to weight-average molecular weights M_z/M_w determined from sedimentation equilibrium data[3] for samples X6-4-4, X8-3-5, and X8-3-8 were 1.1_5, 1.1_4, and 1.1_6, respectively.

Light Scattering. Light scattering on samples X5-8 and X6-4-7 in 0.1 M aqueous NaCl at 25 °C was studied with a Fica 50 light scattering photometer in an angular range θ from 22.5 to 150°. Vertically polarized incident light of 436- or 546-nm wavelength was used. The experimental procedures and data analysis employed were the same as those described previously.[3]

As was found in our previous study,[3] Na salt xanthan dissolves in cadoxen [tris(ethylenediamine)cadmium dihydroxide] as single flexible chains. Light scattering measurement was also made on samples X5-8 and X6-4-7 in this solvent to check whether, as found previously,[3] M_w(in 0.1 M NaCl)/M_w(in cadoxen) for either sample comes close to 2.

Sedimentation Velocity. Sedimentation velocity measurements on all 12 Na salt xanthan samples in 0.1 M aqueous NaCl at 25 °C were carried out in a Beckman Model E ultracentrifuge, using a Kel-F 30-mm single-sector cell. The rotor speed chosen was 44 000 or 48 000 rpm. Sedimentation coefficients s for a series of initial polymer mass concentrations c_0 were determined by the usual peak method and analyzed by the equation $s^{-1} = s_0^{-1}(1 + k_s c_0)$ to obtain the limiting sedimentation coefficient s_0 and the constant k_s.

Table I
Results from Light Scattering Measurements on Na Salt Xanthan Samples in 0.1 M Aqueous NaCl at 25 °C

sample	$M_w \times 10^{-4}$	$A_2 \times 10^4$/(cm^3 mol g^{-2})	$\langle S^2 \rangle^{1/2}$/ nm	M_w (in 0.1 M NaCl) / M_w (in cadoxen)
X4-5	740	3.17	378	2.08
X5-6	394	2.91	257	2.01
X5-8	256	3.08	208	1.83
X3-5	142	3.99	142	1.91
X9-3	99.4	3.79	108	2.02
X7-3b	60.3	4.35	74.8	2.04
X6-3-7	36.2	4.77	50.8	2.05
X6-4-4	24.0	5.02	36.3	1.97
X10-4	20.9	5.34	34.0	1.90
X6-4-7	16.4	5.64	25.1	1.89
X8-3-5	11.2	6.18	16.6	2.47
X8-3-8	7.40	6.80	$10_{.8}$	2.13

Results

Light Scattering Data. Figures 1 and 2 illustrate, respectively, the concentration dependence of $(Kc/R_0)^{1/2}$

0024-9297/84/2217-2696$01.50/0

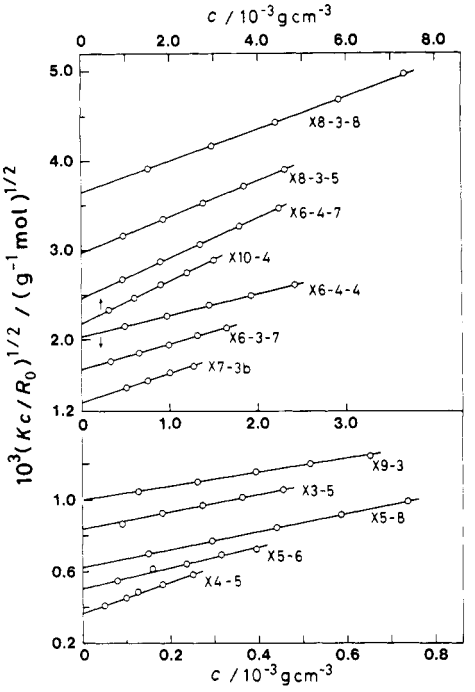

Figure 1. Concentration dependence of $(Kc/R_0)^{1/2}$ for Na salt xanthan samples in 0.1 M aqueous NaCl at 25 °C.

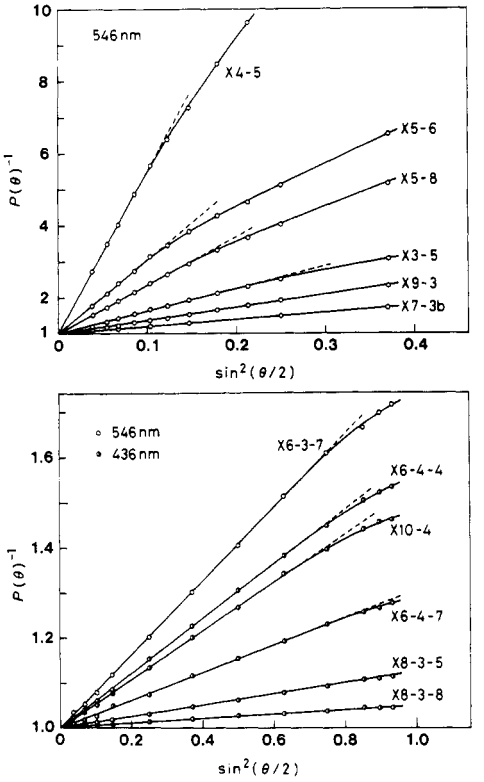

Figure 2. Particle scattering functions for Na salt xanthan samples in 0.1 M aqueous NaCl at 25 °C.

and the angular dependence of the reciprocal of the particle scattering function $P(\theta)^{-1}$ for 12 Na salt xanthan samples in 0.1 M aqueous NaCl at 25 °C. Here, K is the optical constant, c the polymer mass concentration, and R_0 the reduced scattering intensity at zero scattering angle. The values of M_w, A_2 (the second virial coefficient), and $\langle S^2 \rangle^{1/2}$ (the radius of gyration) obtained from the indicated lines are summarized in Table I. The values of M_w(in 0.1 M NaCl)/M_w(in cadoxen), also presented in this table, confirm the previous conclusion[3] that Na salt xanthan in 0.1 M aqueous NaCl consists of paired chains.

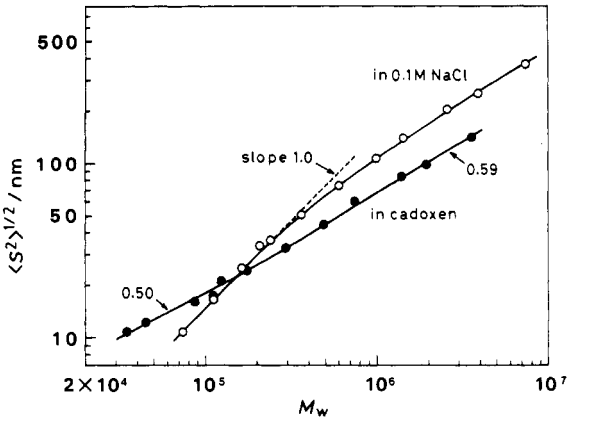

Figure 3. Molecular weight dependence of $\langle S^2 \rangle^{1/2}$ for Na salt xanthan in 0.1 M aqueous NaCl and cadoxen at 25 °C.

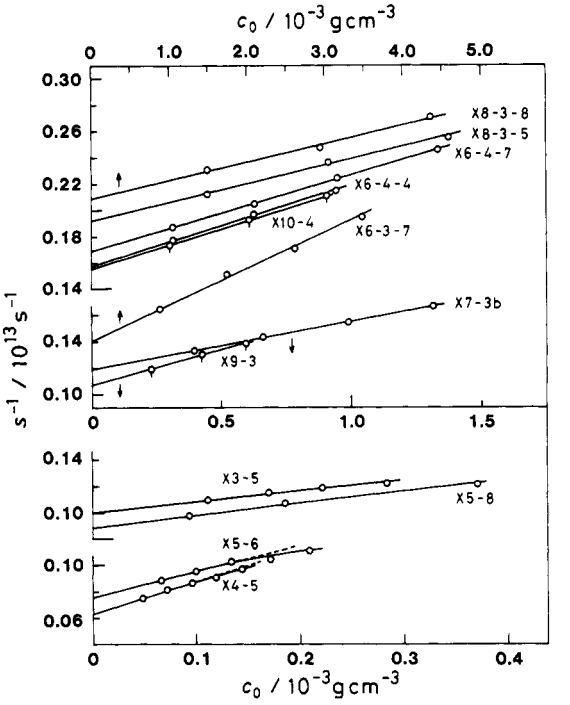

Figure 4. Concentration dependence of s^{-1} for Na salt xanthan samples in 0.1 M aqueous NaCl at 25 °C.

The molecular weight dependence of $\langle S^2 \rangle^{1/2}$ in 0.1 M aqueous NaCl is illustrated in Figure 3, along with that in cadoxen. The slope of the curve for 0.1 M NaCl is about unity in the region of M_w below 3×10^5 and decreases gradually with increasing M_w in the region of higher M_w. Thus, the double helix of xanthan in 0.1 M aqueous NaCl is almost completely rigid below and semiflexible above $M_w \sim 3 \times 10^5$. On the other hand, the slope of the cadoxen curve increases from 0.5 to 0.59 with increasing M_w. This slight change in slope suggests that the single xanthan chain in cadoxen suffers more excluded-volume effect with increasing molecular weight.

Hydrodynamic Data. Figure 4 shows the concentration dependence of s^{-1} for 12 Na salt samples in 0.1 M aqueous NaCl at 25 °C. The values of s_0 and k_s evaluated from the indicated straight lines are presented in Table II.

The molecular weight dependence of s_0 is shown in Figure 5. It can be seen that the values of s_0 for M_w below 4×10^5 vary linearly with log M_w. This behavior of s_0 is consistent with the previous finding from light scattering[3] and viscosity[4] that double-helical xanthan of low molecular weight is essentially rigid and straight. The upswing of

Table II
Results from Sedimentation Velocity and Viscosity Measurements on Na Salt Xanthan Samples in 0.1 M Aqueous NaCl at 25 °C

sample	$s_0 \times 10^{13}$/s	$k_s \times 10^{-2}$/(cm^3 g^{-1})	$[\eta] \times 10^{-2}$/(cm^3 g^{-1})	k'
X4-5	16.1	41.2	90.0	0.46
X5-6	13.3	25.7	51.1	0.42
X5-8	11.4	11.9	35.8	0.43
X3-5	10.0	8.36	18.0	0.42
X9-3	9.35	5.08	10.1	0.37
X7-3b	8.40	3.07	5.75	0.40
X6-3-7	7.14	1.99	3.20	0.39
X6-4-4	6.33	1.15	1.81	0.40
X10-4	6.41	1.15	1.52	0.42
X6-4-7	5.92	1.02	1.06	0.41
X8-3-5	5.21	0.74	0.608	0.46
X8-3-8	4.74	0.62	0.350	0.50

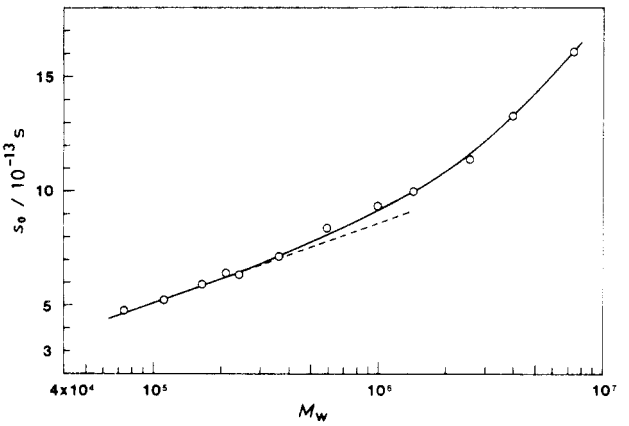

Figure 5. Plot of s_0 vs. log M_w for Na salt xanthan in 0.1 M aqueous NaCl at 25 °C.

s_0 for higher M_w is also consistent with the finding from $\langle S^2\rangle^{1/2}$ data that the helix for M_w higher than about 3×10^5 is no longer rigid but semiflexible.

The fourth and fifth columns of Table II present the values of $[\eta]$ (the zero-shear-rate intrinsic viscosity) and k' (the Huggins constant) for 12 xanthan samples in 0.1 M aqueous NaCl at 25 °C.

Discussion

Double-Stranded Helical Structure. The well-known expressions for $\langle S^2\rangle^{1/2}$ and s_0 of a long, straight cylinder[7] are

$$\langle S^2\rangle^{1/2} = (1/12)^{1/2}(M/M_L) \quad (1)$$

$$s_0 = \frac{(1-\bar{v}\rho_0)M_L}{3\pi\eta_0 N_A}[\ln M + 0.3863 - \ln(dM_L)] \quad (2)$$

where M is the polymer molecular weight, M_L the molar mass per unit contour length of the cylinder, $\bar{v}$ the partial specific volume of the polymer, ρ_0 the solvent density, η_0 the solvent viscosity, N_A Avogadro's constant, and d the diameter of the cylinder; the buoyancy factor $1 - \bar{v}\rho_0$ for Na salt xanthan in 0.1 M aqueous NaCl at 25 °C is 0.401.[3]

Substitution of our $\langle S^2\rangle^{1/2}$ data for M_w below 3×10^5 in 0.1 M aqueous NaCl into eq 1 yields 1940 ± 50 nm^{-1} for M_L. Further, when compared with eq 2, the linear relation between s_0 and log M_w in Figure 5 leads to $M_L = 1940 \pm 80$ nm^{-1} and $d = 2.7 \pm 0.5$ nm. The agreement of the M_L values from $\langle S^2\rangle$ and s_0 is very satisfactory.[8] The d value of 2.7 nm from s_0 is somewhat larger than the values 2.0–2.5 nm estimated previously[4] from $[\eta]$.

Table III
Pitch per Residue, Diameter, and Persistence Length of the Xanthan Double Helix in 0.1 M Aqueous NaCl

h/nm	d/nm	q/nm	method
0.47 ± 0.02		120 ± 10	light scattering
0.47 ± 0.02	2.7 ± 0.5	130 ± 20	sedimentation
	2.2 ± 0.3[a]	100 ± 20	viscosity
0.47	1.9		X-ray[b]
	2.2		molecular model[b]

[a] Previous estimate.[4] [b] Reference 5.

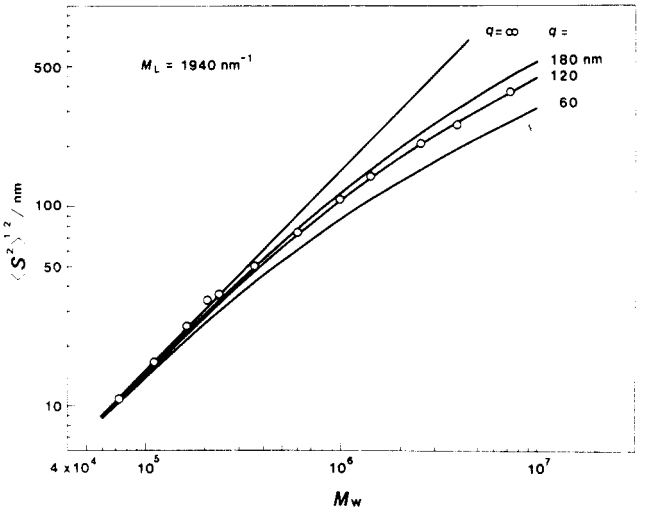

Figure 6. Comparison between the measured $\langle S^2\rangle^{1/2}$ (in 0.1 M aqueous NaCl) and the theoretical values calculated from eq 3 for different q with M_L fixed to 1940 nm^{-1}.

The molar mass per glucose residue of Na salt xanthan with DS_{pyr} ranging from 0.32 to 0.37 is 460 ± 1 g mol^{-1}. With this and the M_L estimated above from either light scattering or sedimentation data, the pitch h per main-chain glucose residue of the xanthan double helix is evaluated to be 0.47 ± 0.02 nm.

The h and d values from our solution studies are compared in Table III with the h and d estimated from Okuyama et al.'s crystallographic data and molecular model[5] for xanthan. The close agreement in h and d from two different sources confirms our previous conclusion[3,4] that the double-helical structure of xanthan in 0.1 M aqueous NaCl is essentially the same as that in the crystalline state. It is to be noted that the d values of 2.4 ± 0.3 nm (the average of the two estimates from our $[\eta]$ and s_0 data) and 2.1 ± 0.2 nm (from Okuyama et al.'s crystallographic data and molecular model) are almost half the value 4 nm estimated by Holzwarth and Prestridge[12] from electron micrographs.

Rigidity of the Double Helix. As mentioned above, xanthan double helices with M_w higher than about 3×10^5 in 0.1 M aqueous NaCl are semiflexible. A typical model for semiflexible polymers is the Kratky–Porod wormlike chain,[13] whose rigidity is defined by the persistence length q. The Benoit–Doty expression[14] for $\langle S^2\rangle$ of this model chain in the unperturbed state is

$$\langle S^2\rangle = (qM/3M_L) - q^2 + (2q^3M_L/M)[1 - (qM_L/M)(1 - e^{-M/qM_L})] \quad (3)$$

A trial-and-error method was used to find a q value which leads to the closest agreement between our $\langle S^2\rangle^{1/2}$ data and eq 3 with M_L fixed to 1940 nm^{-1}. It is shown in Figure 6 that eq 3 with $q = 120$ nm gives the best fit to the data points. When M_L was allowed to vary within the

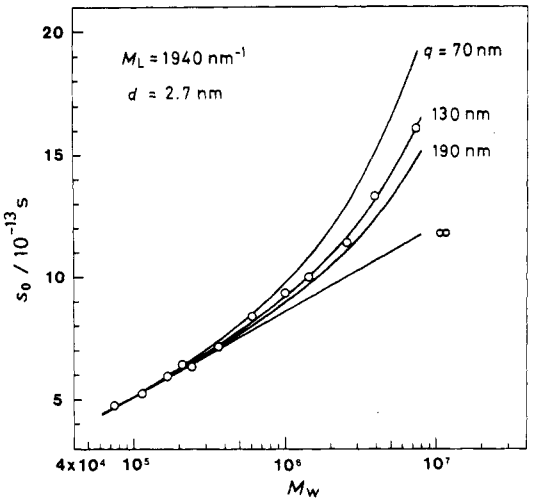

Figure 7. Comparison between the measured s_0 and the Yamakawa–Fujii theoretical values calculated for different q with M_L and d fixed to 1940 nm^{-1} and 2.7 nm, respectively.

range of uncertainty ± 50 nm^{-1} (see above), q changed from 110 to 130 nm.

The Yamakawa–Fujii theory[7] for s_0 of an unperturbed wormlike cylinder contains M_L, q, and d as parameters. Figure 7 shows that when M_L and d are fixed, respectively, to 1940 nm^{-1} and 2.7 nm, a q of 130 nm gives the best agreement between our s_0 data and the Yamakawa–Fujii theoretical values.

In a previous paper,[4] our $[\eta]$ data in 0.1 M aqueous NaCl were shown to fit the Yamakawa–Fujii–Yoshizaki theory[15,16] for unperturbed wormlike cylinders, provided M_L = 1940 nm^{-1}, q = 120 nm, both derived from $\langle S^2\rangle^{1/2}$ data for six samples, and d = 2.0–2.5 nm. We here reevaluate d and q from the more extensive $[\eta]$ data given in Table II, taking M_L to be 1940 ± 50 nm^{-1} as determined above from $\langle S^2\rangle$ or s_0 data and using the plot of $(M_w^2/[\eta])^{1/3}$ vs. $M_w^{1/2}$ proposed by Bushin et al.[17] and Bohdaneckŷ.[18]

This plot constructed from our data is shown in Figure 8a. The data points for $M_w^{1/2} > 500$ follow a straight line whose intercept I and slope S are equal to 450 ± 10 and 0.49 ± 0.02 g$^{1/3}$ cm^{-1}, respectively. According to Bohdaneckŷ's analysis,[18] I and S are related to M_L, d, and q by

$$I = 1.516 \times 10^{-8} A_0 M_L \quad (g^{1/3}\ cm^{-1}) \qquad (4)$$

$$S = 1.516 \times 10^{-8} B_0 (2q/M_L)^{-1/2} \quad (g^{1/3}\ cm^{-1}) \qquad (5)$$

where A_0 and B_0, functions of $d/2q$, are tabulated in his paper. Substitution of the above I and S values and the M_L value of 1940 ± 50 nm^{-1} into eq 4 and 5 yields 2.2 ± 0.5 nm for d and 100 ± 20 nm for q. The former confirms the estimate, 2.0–2.5 nm, from our previous $[\eta]$ data,[4] while the latter is somewhat smaller than 120 nm from $\langle S^2\rangle$ and 130 nm from s_0.

Figure 8b shows that our $[\eta]$ data are fitted accurately by the Yamakawa–Fujii–Yoshizaki theoretical curve calculated for M_L = 1940 nm^{-1}, d = 2.2 nm, and q = 100 nm. The fit is clearly closer than what we found previously[4] with q = 120 nm and the same values taken for M_L and d (the dot–dash line in Figure 8b).

The q values estimated above from $\langle S^2\rangle$, s_0, and $[\eta]$ data (see Table III) are within ±20 nm of 120 nm. This fair agreement in q leads to the conclusion that our light scattering, sedimentation, and viscosity data in 0.1 M aqueous NaCl are all consistent with one another throughout the entire range of molecular weight studied.

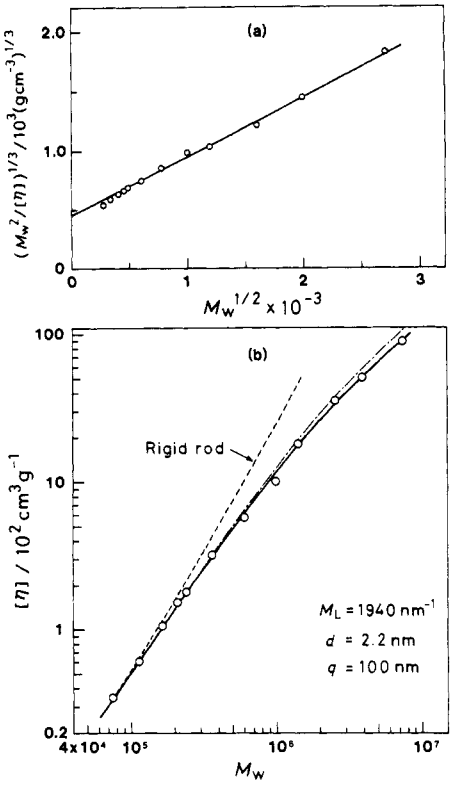

Figure 8. (a) Plot of $(M_w^2/[\eta])^{1/3}$ vs. $M_w^{1/2}$ for Na salt xanthan in 0.1 M aqueous NaCl at 25 °C. (b) Comparison between the measured $[\eta]$ and the Yamakawa–Fujii–Yoshizaki theoretical values (the solid line) for M_L = 1940 nm^{-1}, d = 2.2 nm, and q = 100 nm. Dot–dash line, q = 120 nm; dashed line, $q = \infty$.

The rigidity of the xanthan double helix in 0.1 M aqueous NaCl, characterized by a q of 120 ± 20 nm, is intermediate between those of double-stranded DNA[19,20] (60 nm) and triple-stranded collagen[21] or schizophyllan[22,23] (150–200 nm).

References and Notes

(1) Jansson, P. E.; Kenne, L.; Lindberg, B. *Carbohydr. Res.* **1975**, *45*, 275.
(2) Melton, L. D.; Mindt, L.; Rees, D. A.; Sandersson, G. R. *Carbohydr. Res.* **1976**, *46*, 245.
(3) Sato, T.; Norisuye, T.; Fujita, H. *Polym. J.* **1984**, *16*, 341.
(4) Sato, T.; Kojima, S.; Norisuye, T.; Fujita, H. *Polym. J.* **1984**, *16*, 423.
(5) Okuyama, K.; Arnott, S.; Moorhouse, R.; Walkinshow, M. D.; Atkins, E. D. T.; Wolf-Ullish, Ch. In "Fiber Diffraction Methods"; French, A. D., Gardner, K. H., Eds.; American Chemical Society: Washington, DC, 1980; ACS Symp. Ser. No. 141, p 411.
(6) See ref 3 for the determination of DS_{pyr}.
(7) Yamakawa, H.; Fujii, M. *Macromolecules* **1973**, *6*, 407.
(8) Our M_L value of 1940 nm^{-1} happens to be very close to 2000 nm^{-1} obtained by Holzwarth[9] and Paradossi and Brant[10] respectively from hydrodynamic data and asymptotic $P(\theta)$ and is about twice as large as 1000 nm^{-1} estimated by Rinaudo and Milas[11] from dimensional and hydrodynamic data for one sample. However, these M_L values of other authors were estimated on certain assumptions as noted in our previous papers[3,4] and hence cannot be regarded as directly measured values.
(9) Holzwarth, G. *Carbohydr. Res.* **1978**, *66*, 173.
(10) Paradossi, G.; Brant, D. A. *Macromolecules* **1982**, *15*, 874.
(11) Rinaudo, M.; Milas, M. *Biopolymers* **1978**, *17*, 2663.
(12) Holzwarth, G.; Prestridge, E. B. *Science (Washington, D.C.)* **1977**, *197*, 757.
(13) Kratky, O.; Porod, G. *Recl. Trav. Chim. Pays-Bas* **1949**, *68*, 1106.
(14) Benoit, H.; Doty, P. *J. Phys. Chem.* **1953**, *57*, 958.
(15) Yamakawa, H.; Fujii, M. *Macromolecules* **1974**, *7*, 128.
(16) Yamakawa, H.; Yoshizaki, T. *Macromolecules* **1980**, *13*, 633.
(17) Bushin, S. V.; Tsvetkov, V. N.; Lysenko, E. B.; Emelyanov, V. N. *Vysokomol. Soedin., Ser. A* **1981**, *A23*, 2494.

(18) Bohdanecký, M. *Macromolecules* **1983**, *16*, 1483.
(19) Record, M. T., Jr.; Woodbury, C. P.; Inman, R. B. *Biopolymers* **1975**, *14*, 393.
(20) Godfrey, J. E.; Eisenberg, H. *Biophys. Chem.* **1976**, *5*, 301.
(21) Saito, T.; Iso, N.; Mizuno, H.; Onda, N.; Yamato, H.; Odashima, H. *Biopolymers* **1982**, *21*, 715.
(22) Yanaki, T.; Norisuye, T.; Fujita, H. *Macromolecules* **1980**, *13*, 1462.
(23) Kashiwagi, Y.; Norisuye, T.; Fujita, H. *Macromolecules* **1981**, *14*, 1220.

Elementary Processes in Side-Chain Motions of Poly(α-amino acids)

Shin Yagihara, Ryusuke Nozaki, and Satoru Mashimo*

Department of Physics, Faculty of Science, Tokai University, Hiratsuka-shi, Kanagawa 259-12, Japan

Kunio Hikichi

Department of Polymer Science, Faculty of Science, Hokkaido University, Sapporo 060, Japan. *Received February 22, 1984*

ABSTRACT: Dielectric measurements covering a frequency range from 10 MHz up to 10 GHz were performed on poly(γ-methyl L-glutamate), poly(γ-benzyl L-glutamate), and poly[γ-(*p*-chlorobenzyl) L-glutamate] in dioxane solution at 25 °C by means of time-domain reflectometry. Two relaxation processes with relaxation times around 440 and 20 ps were observed for each polymer. The lower frequency relaxation process can be attributed to restricted rotations of C–C bonds in the side chain, neighboring to the α-helical backbone. The higher frequency process is caused by free rotations of C–O bonds in the side chain.

I. Introduction

Physical and chemical properties of poly(α-amino acids) have been studied extensively as simple models of proteins and rodlike molecules. It has been pointed out that side chains play important roles in chain conformations of protein molecules.[1-3] There remains a great interest in understanding the side-chain motions of synthetic analogues.

A number of investigations of the side-chain motions of poly(α-amino acids) have been made in the solid state by the dielectric method. An important result of these studies is that only one relaxation process is observed, even if the side chains have several dipole components.[4-7] A reasonable interpretation is that the process results from cooperative motions of neighboring side chains. Observation of a single-relaxation process in some copolymers supports strongly existence of cooperative motions.[4,5] A detailed discussion of cooperative motions has been given elsewhere.[6]

Recently, Nakamura et al.[8] found a side-chain relaxation process of poly(γ-benzyl L-glutamate) (PBLG) in dioxane solution, the relaxation time of which is about 150 ps at 20 °C by the time-domain reflectometry (TDR) method. However, cooperative interactions between neighboring side chains are thought to be weaker in dilute solution than in the solid state. Therefore, in order to examine whether multiple relaxation processes according to various kinds of localized motions in the side chain exist or not, relaxation measurements over a wide and high frequency region have long been desired.

Recent developments in the TDR method are remarkable and make it possible to measure the complex permittivity easily even at 10 GHz.[9-11] Single-bond rotations in some oxide polymers have already been observed in the gigahertz region by the TDR method.[10] Employing the TDR method in this work, we performed dielectric measurements on poly(γ-methyl L-glutamate) (PMLG), PBLG, and poly[γ-(*p*-chlorobenzyl) L-glutamate] (PpClBLG) in dioxane solutions in order to clarify elementary processes of their side-chain motions.

Table I
Relaxation Parameters for Poly(α-amino acids) in Dioxane Solution at 25 °C[a]

	lower frequency process			higher frequency process		
sample	τ_l, ps	$\Delta\epsilon_l$	μ_{el}, D	τ_h, ps	$\Delta\epsilon_h$	μ_{eh}, D
PMLG	480	0.028	0.92	16	0.054	1.3
PBLG	430	0.049	1.1	22	0.040	1.0
PpClBLG	420	0.033	1.0	20	0.077	1.6

[a] Concentrations are 2.5 wt % for PMLG and 5 wt % for the others.

II. Experimental Section

PMLG (Ajicoat A-2000) was provided by Ajinomoto Co., Ltd. PBLG was obtained from Sigma Co., Ltd. PpClBLG was prepared by the ester-exchange reaction of PMLG and *p*-chlorobenzyl alcohol.[6,12] The mole fraction of *p*-chlorobenzyl glutamate was determined as 99% from proton NMR spectra. The concentrations of the polymers in dioxane solution used were 2.5 wt % for PMLG and 5 wt % for both PBLG and PpClBLG.

Dielectric measurements were made in the frequency range 10 MHz to 10 GHz at 25 °C by the TDR method. The apparatus and detailed procedures have already been reported.[10] We used a cell with a length of the inner conductor d = 0.402 mm for measurements at frequencies lower than 1 GHz, and a cell with d = 0.128 mm at frequencies higher than 0.5 GHz. Effective lengths γd for these cells are 1.92 and 1.11 mm, respectively.

III. Results

Figures 1–3 show frequency dependences of the complex permittivity for the PMLG, PBLG, and PpClBLG solutions, respectively. Two relaxation processes are found in each polymer solution. Nakamura et al.[8] pointed out that relaxations observed in such a high-frequency region must reflect the side-chain motions.

In order to obtain relaxation parameters for each process, the permittivity ϵ^* ($=\epsilon' - j\epsilon''$) is assumed to be given as a superposition of two single-relaxation processes[13]

$$\epsilon^* = \epsilon_\infty + \frac{\Delta\epsilon_l}{1 + j\omega\tau_l} + \frac{\Delta\epsilon_h}{1 + j\omega\tau_h} \quad (1)$$

where ϵ_∞ is the high-frequency limit of the permittivity,

0024-9297/84/2217-2700$01.50/0